



HAL
open science

Evaluation of proton density fat fraction (PDFF) obtained from a vendor-neutral MRI sequence and MRQuantif software

Thibaud Orcel, H. T. Chau, Bruno Turlin, Julien Chaigneau, Elise Bannier, Philippe Otal, Eric Frampas, Arnaud Leguen, Anne Boulic, Hervé Saint-Jalmes, et al.

► To cite this version:

Thibaud Orcel, H. T. Chau, Bruno Turlin, Julien Chaigneau, Elise Bannier, et al.. Evaluation of proton density fat fraction (PDFF) obtained from a vendor-neutral MRI sequence and MRQuantif software. *European Radiology*, 2023, 33 (12), pp.8999-9009. 10.1007/s00330-023-09798-4. hal-04192082

HAL Id: hal-04192082

<https://hal.science/hal-04192082v1>

Submitted on 26 Oct 2023

HAL is a multi-disciplinary open access archive for the deposit and dissemination of scientific research documents, whether they are published or not. The documents may come from teaching and research institutions in France or abroad, or from public or private research centers.

L'archive ouverte pluridisciplinaire **HAL**, est destinée au dépôt et à la diffusion de documents scientifiques de niveau recherche, publiés ou non, émanant des établissements d'enseignement et de recherche français ou étrangers, des laboratoires publics ou privés.



Distributed under a Creative Commons Attribution - NonCommercial 4.0 International License

Evaluation of proton density fat fraction (PDFF) obtained from a vendor-neutral MRI sequence and MRQuantif software.

Orcel T (1), Chau HT (1), Turlin B (2, 3), Chaigneau J (4), Bannier E (1, 5), Otal P (6), Frampas E (7), Leguen A (8), Boulic A (9), Saint-Jalmes H (10), Aubé C (4,11), Boursier J (4,12), Bardou-Jacquet E (3,13), Gandon Y (1,3)

ORCEL T and CHAU HT are first authors.

- (1) Department of Radiology, Rennes University Hospital, 2 rue H. Le Guilloux, 35033, Rennes, France
- (2) Department of Pathology, Rennes University Hospital, 2 rue H. Le Guilloux, 35033, Rennes, France
- (3) NUMECAN, INSERM U1099, Rennes University Hospital, 2 rue H. Le Guilloux, 35033, Rennes, France
- (4) HIFIH, UPRES EA 3859, Angers University Hospital, 4 Rue Larrey, 49993, Angers, France
- (5) EMPENN U746 Unit/Project, INSERM/INRIA, IRISA, UMR CNRS 6074, University of Rennes, Beaulieu Campus, 35042, Rennes, France
- (6) Department of Radiology, Toulouse University Hospital, 1 Av Pr J. Poulhes, 31059, Toulouse, France
- (7) Department of Radiology, Nantes University Hospital, 1 Pl. Alexis-Ricordeau, 44000, Nantes, France
- (8) Department of Radiology, Bretagne-Atlantique Hospital, 20 Bd Général Maurice Guillaudot, 56000, Vannes, France
- (9) Department of Radiology, Bretagne Sud Hospital, 5 avenue de Choiseul, 56322, Lorient, France
- (10) LTSI, INSERM U1099, University of Rennes, Beaulieu Campus, 35042, Rennes, France
- (11) Department of Radiology, Angers University Hospital, 4 Rue Larrey, 49993, Angers, France
- (12) Department of Hepatology-Gastroenterology, Angers University Hospital, 4 Rue Larrey, 49993, Angers, France
- (13) Department of Hepatology, Rennes University Hospital, 2 rue H. Le Guilloux, 35033, Rennes, France

Corresponding author :

Prof Yves GANDON
Departement of Radiology
Hôpital Pontchaillou
Rue H Le Guilloux
35033 Rennes CEDEX
France

Email : yves.gandon@chu-rennes.fr

Mobile : +33 6 88 67 44 14

Fax : +33 2 99 28 43 64

Evaluation of proton density fat fraction (PDFF) obtained from a vendor-neutral MRI sequence and MRQuantif software.

Abstract

Objective:

To validate the proton density fat fraction (PDFF) obtained by the MRQuantif software from 2D chemical shift encoded MR (CSE-MR) data in comparison with the histological steatosis data.

Methods:

This study, pooling data from 3 prospective studies spread over time between January 2007 and July 2020, analyzed 445 patients who underwent 2D CSE-MR and liver biopsy. MR derived liver iron concentration (MR-LIC) and PDFF was calculated using the MRQuantif software. The histological standard steatosis score (SS) served as reference. In order to get a value more comparable to PDFF, histomorphometry fat fraction (HFF) were centrally determined for 281 patients. Spearman correlation and the Bland and Altman method were used for comparison.

Results:

Strong correlations were found between PDFF and SS ($r_s=0.84$, $p<0.001$) or HFF ($r_s=0.87$, $p<0.001$). Spearman's coefficients increased to 0.88 ($n=324$) and 0.94 ($n=202$) when selecting only the patients without liver iron overload. The Bland and Altman analysis between PDFF and HFF found a mean bias of $5.4\% \pm 5.7$ [CI95% 4.7, 6.1]. The mean bias was $4.7\% \pm 3.7$ [CI95% 4.2, 5.3] and $7.1\% \pm 8.8$ [CI95% 5.2, 9.0] for the patients without and with liver iron overload, respectively.

Conclusion:

The PDFF obtained by MRQuantif from a 2D CSE-MR sequence is highly correlated with the steatosis score and very close to the fat fraction estimated by histomorphometry. Liver iron overload reduced the performance of steatosis quantification and joint quantification is recommended. This device-independent method can be particularly useful for multicenter studies.

1 **Key words**

- 2
- 3
- 4 1. Magnetic resonance imaging,
- 5 2. non-alcoholic fatty liver disease,
- 6 3. non-alcoholic steatohepatitis,
- 7 4. liver biopsy.
- 8
- 9

10

11

12 **Key points:**

- 13
- 14 • The PDFF measured by MRQuantif from 2D CSE–MR sequence data is highly
- 15 correlated to hepatic steatosis.
- 16
- 17 • Steatosis quantification performance is reduced in case of significant hepatic iron
- 18 overload.
- 19
- 20 • This vendor-neutral method may allow consistent estimation of PDFF in multicenter
- 21 studies.
- 22

23 **Clinical Relevance statement**

24

25 The quantification of liver steatosis using a vendor-neutral 2D chemical-shift MR sequence,

26 processed by MRQuantif, is well correlated to steatosis score and histomorphometric fat

27 fraction obtained from biopsy, whatever the magnetic field and the MR device used.

28

29

30

31

32

33 **Abbreviation**

34

35 BMI: body mass index

36 CI: confidence interval

37 CRN: clinical research network

38 CSE–MR: chemical shift encoded magnetic resonance

39 FF: fat fraction

40 HFF: histomorphometry fat fraction

41 LIC: liver iron concentration

42 MR–LIC: MR-derived liver iron concentration

43 NAFLD: non-alcoholic fatty liver disease

44 NASH: non-alcoholic steatohepatitis

45 SS: steatosis score

46 WIP: work in progress version

47

48

49

50

51

52

53

54

55

56

57

58

59

60

61

62

63

64

65

Introduction

1
2
3
4 Non-alcoholic fatty liver disease (NAFLD) is the most common chronic liver disease
5 worldwide and a major healthcare problem, with a global prevalence reaching 20 to 30 % of
6 the population in America, Europe or Middle east [1, 2]. A small proportion (2 to 3%) develops
7 a non-alcoholic steatohepatitis (NASH) which can progress into liver cirrhosis and
8 hepatocellular carcinoma [1]. Thus, the quantification of the fat content of the liver is becoming
9 a major biomarker for the management of these patients.
10
11
12
13
14
15

16 For this purpose, the classical gold standard reference is liver biopsy but there are some
17 contraindications or limitations [3, 4]. It is also a painful procedure with potential complication,
18 such as intraabdominal bleeding. On liver biopsy, estimation of fat is classically performed with
19 the use of a semi quantitative scoring system developed by the NASH Clinical Research
20 Network (CRN) [5]. This scoring subjectively counts the percentage of hepatocytes containing
21 lipid vacuoles. To obtain a truly quantitative fat fraction, some previous studies used
22 quantitative methods so called histomorphometry or stereological analysis [6, 7]. In comparison
23 to the histological scoring, area of steatosis determined by histomorphometry had a good
24 reliability with a better accuracy and reproducibility [8].
25
26
27
28
29
30
31
32
33

34 To avoid biopsy, non-invasive imaging methods have been evaluated. Ultrasonography or
35 computed tomography are less accurate than magnetic resonance imaging or spectroscopy [9].
36 Magnetic resonance spectroscopy was initially considered as the method of choice for non-
37 invasive hepatic lipid content determination and correlated well with liver biopsy, but is not
38 effectively used in daily routine, due to its low availability and limited clinical application [9,
39 10]. More simple magnetic resonance imaging advanced techniques based on chemical shift
40 encoded MR sequences (CSE-MR) have been developed to measure proton density fat fraction
41 (PDFF). There are several confounders for PDFF quantification: T1 relaxation, T2* relaxation
42 effects and the spectral complexity of fat [11, 12]. They can be reduced by using a small flip
43 angle, by taking into account the T2* decay and also by using a multipeak fat signal model [13–
44 16]. With these strategies, PDFF is accurate compared to magnetic resonance spectroscopy
45 results [17, 18] and also to the histological score [19–21]. It also has an excellent linearity and
46 precision, with a limited bias, across different field strengths, imager manufacturer and
47 reconstructions models [22].
48
49
50
51
52
53
54
55
56
57
58
59
60
61
62
63
64
65

1 Each MRI vendor proposes a dedicated sequence, with specific parameters (TR, TE, number of
2 TEs, flip angle ...) processed by a proprietary algorithm to evaluate simultaneously PDFF and
3 R2*, a surrogate of liver iron concentration. There is overall good reproducibility but with
4 potential vendor bias, at least in phantoms [23]. A vendor-neutral 2D chemical shift encoded
5 MR (CSE-MR) sequence can also be used. R2* and PDFF can be calculated by external
6 software such as MRQuantif which is a research software developed by the Rennes University
7 Hospital and freely available on the internet (<http://imageded.univ-rennes1.fr/mrquantif>).
8 Because it has been validated against biochemical liver iron concentration determined from
9 biopsy, it is widely used worldwide to quantify liver iron concentration (MR-LIC). However,
10 PDFF results provided have not been evaluated in comparison to biopsy.
11
12
13
14
15
16
17
18
19
20

21 The purpose of this study is to determine if this method can also be used to accurately quantify
22 liver fat on various MR devices.
23
24
25
26
27

28 **Methods**

29 **Patient population**

30 This study pooled data from one cohort (SNIFF) approved by Commission nationale de
31 l'informatique et des libertés (CNIL) N°1998-001 and 2 prospective multicenter studies (Surfer
32 NCT00401336 and FibroMR NCT03245606) in which liver MRI and liver biopsy were
33 performed for suspicion of NASH except in the Surfer study in which biopsy could also have
34 been indicated in a clinico-biological context of liver iron overload. These 3 studies were
35 approved by the institutional review board (IRB) of the corresponding sponsor institution. All
36 patients provided written informed consent for liver biopsy and hepatic MR examination. They
37 were included between January 2007 and July 2020.
38
39
40
41
42
43
44
45
46
47
48

49 A total of 450 patients, examined in 9 different centers were recruited. After excluding 2
50 patients with inadequate MR results and 14 patients with more than 30 days between MRI and
51 biopsy, 434 patients were retained for analysis.
52
53
54
55
56

57 Age, sex and BMI were recorded for all patients.
58
59
60
61
62
63
64
65

Magnetic resonance imaging protocol

MR studies were obtained from 11 different MRI scanners, 6 with a 3 T magnetic field: Signa Pioneer from GE Healthcare, Achieva or Ingenia from Philips, Verio, Prisma or Skyra from Siemens, and 5 with a 1.5T field: Signa HDxt (GE), Achieva or Ingenia (Philips), and Aera or Avanto (Siemens).

Each MR study included, at least, a 2D CSE–MR sequence, proposed by the University of Rennes website and compatible with the MRQuantif software processing. The repetition time was set to 120 ms and the flip angle to 20° in order to minimize the T1 effect. As recommended by the website instructions, the sequence was performed using the system body coil only. The sequence included 10 to 12 echoes with TEs multiple of 1.2 ms, with the exception of two 1.5T devices which used multiple of 2.4 ms. A minimum of 3 slices was obtained in the middle part of the liver. Slice thickness ranged between 7 and 10 mm, and slice center interval varied from 10 mm to 23 mm. Detailed parameters are provided in supplementary material.

In one center, in the most recent study, 43 patients were explored, on a Magnetom Prisma MR-scanner (Siemens), with 3 additional sequences: a 2D CSE–MRI with multi-channel array coils instead of the body coil, a 3D VIBE q–Dixon from the LiverLab package and a work-in-progress (WIP) VIBE q-Dixon version.

All sequences were obtained without contrast agent injection, in a 15 – 20s breath-hold and in the axial plane.

MRI data analysis

Signal intensity measurement was performed on magnitude images using the MRQuantif software by one experienced abdominal radiologist blinded to either clinical record and histological results. Three ROI of 5 cm² were placed on a user-selected slice in the right liver lobe, avoiding the marginal region, lung susceptibility artifacts, large intrahepatic vessels and any obvious motion-affected regions. Two ROI of 1.8cm² were placed one on the right and one in the left paraspinal muscles to be used as comparison reference for the iron quantification process. One last ROI of 5 cm² was placed outside of the body, in order to measure the background noise, useful for R2* calculation. All ROIs were automatically propagated to all images with the different TEs at the same slice location. The placement of each ROI is illustrated in Figure 1.

1 MRQuantif (2021.02.08 version) calculated the mean signal intensity values from each ROI. A
2 signal cutoff of twice the noise measurement was applied where applicable. R2* and PDFF
3 were obtained using simplex non-linear algorithm to fit the signal from all echoes to a signal
4 model containing proton density, PDFF, and a common R2* for water and fat. The fat signal
5 model used the resonance frequencies and the percentage of the 3 mean peaks as described by
6 Hamilton [12]. So, the calculation used formula:
7
8
9
10
11

$$12 \quad s(t_n) = A \left| (1 - PDFF) + PDFF \sum_{m=1}^P \alpha_m e^{j2\pi t_n f_m} \right| e^{-t_n R2^*}$$

13
14
15
16
17
18
19
20 s = signal at echo time t_n
21 A = total proton signal
22 P = peaks of fat
23 α_m = relative amplitude of the m peak
24 f_m = frequency of the m peak
25 $PDFF$ = proton density fat fraction
26
27
28

29 The final values of PDFF and R2* corresponded to the mean of the results obtained from the 3
30 liver ROIs. In the MRQuantif preferences section, we chose to convert R2* into MR-LIC using
31 the formula named "standard", proportional to the magnetic field, and to express the results in
32 $\mu\text{mol} / \text{g}$ (upper normal limit = $36\mu\text{mol/g}$). When several series were obtained, an automatic
33 geometric coregistration allowed an identical positioning of the ROIs. This allowed obtaining,
34 at a similar location, mean values of PDFF from the calculated fat fraction map provided by the
35 VIBE q-Dixon sequences.
36
37
38
39
40
41
42

43 **Biopsy analysis**

44 Percutaneous core liver biopsy was obtained following guidelines of the American Association
45 for the study of liver diseases, within right liver lobe, using a 16 Gauge needle. Liver biopsy
46 histological sections were stained in hematoxylin-eosin (H&E) and Sirius red coloration. An
47 experienced liver pathologist, blinded to clinical information and MRI data, reviewed all biopsy
48 samples. He determined a steatosis score (SS) corresponding to the proportion of hepatocytes
49 containing fat vesicles and using near continuous percentage scale, with 5% steps. Grades were
50 defined using the NASH CRN classification: grade 0 with SS < 5%, grade 1 with SS 5 – 33%,
51 grade 2 with SS 33 – 66%, grade 3 with SS > 66% [5].
52
53
54
55
56
57
58
59
60
61
62
63
64
65

1
2
3
4
5
6
7
8
9
10
11
12
13
14
15
16
17
18
19
20
21
22
23
24
25
26
27
28
29
30
31
32
33
34
35
36
37
38
39
40
41
42
43
44
45
46
47
48
49
50
51
52
53
54
55
56
57
58
59
60
61
62
63
64
65

In order to get a quantitative comparable fat fraction from biopsies, specimen slides were sent, when it was possible, to a central laboratory (HIFIH, Angers University). HIFIH previously developed histomorphometric fat fraction (HFF) measurement by morphometry on liver biopsies stained with picosirius red solution [8]. A digital slide scanner (Scanscope CS2 System, Aperio Technologies) was used to generate high quality images (30 000 x 30 000 pixels) at a resolution of 0.5 $\mu\text{m}/\text{pixel}$ (magnification x20). Then, HFF corresponding to the area percentage of the lipid vacuoles, was automatically measured by a dedicated software on the complete liver biopsy sections. For this present work, a cross validation between picosirius red staining and HES staining was performed to also measure HFF when only HES staining was available.

Statistical analysis

Categorical variables were expressed as numbers and percentages. Continuous variables were expressed as means \pm standard deviation (range) if normally distributed, and medians (range, interquartile range) if not normally distributed. Given that PDFF quantitative variables were not normally distributed, the Spearman correlation coefficient (r_s) was calculated in order to estimate the strength of the relation between PDFF and steatosis score, and between PDFF and HFF. The graphic comparison between PDFF and SS or HFF, or between PDFF from two different sequences was done using linear correlation. Differences were evaluated by the method of Bland and Altman and the results were expressed as mean difference \pm standard deviation (95% CIs.) Statistical analyses were done using Microsoft Excel (version 16.0.15629.20156).

Results

This study collected data from 434 subjects, 276 male (64%) and 158 female (36%), with a mean age of 55.1 ± 12.2 years (range 18-81). The mean BMI was 31.0 ± 5.5 (19 – 62.1). The time interval between MR imaging and liver biopsy ranged from 0 to 30 days (median 1 day).

Using the NASH CRN grading score for steatosis, the study population was distributed as follows: 51 patients (12%) were grade 0, 201 patients (46%) were grade 1, 112 patients (26%) were grade 2 and 70 patients (16%) were grade 3.

1
2 Only 281 patients had HFF analysis, 214 on sirius red staining, 11 on H&E staining, and 56 on
3 both stainings. HFF median value was 8.2% (0 – 36%, Q1 1.9%, Q3 15.8%). For the 56 patients
4 analysed with both staining, the Bland and Altman analysis of HFF between sirius red and HES
5 staining found a mean difference of -0.7 ± 2 %. (CI95% -1.4%, -0.6%).
6
7
8
9

10 The median MR–LIC was 26.6 $\mu\text{mol/g}$ (0 – 505 $\mu\text{mol/g}$, Q1 21 $\mu\text{mol/g}$, Q3 37 $\mu\text{mol/g}$). A
11 normal MR–LIC was found in 324 patients. Liver iron overload was found in 110 patients with
12 MR–LIC median at 53.0 $\mu\text{mol/g}$ (37 – 505 $\mu\text{mol/g}$, Q1 43 $\mu\text{mol/g}$, Q3 128 $\mu\text{mol/g}$). Among
13 the 281 patients with HFF analysis, 79 had an hemosiderosis with an MR–LIC median at 55.0
14 $\mu\text{mol/g}$ (37 – 505 $\mu\text{mol/g}$, Q1 44 $\mu\text{mol/g}$, Q3 155 $\mu\text{mol/g}$). Flow chart is available in
15 supplementary material.
16
17
18
19
20
21
22

23 For the whole study population, the median PDFF value was 15.0% (-28 – 55%, Q1 7.1%, Q3
24 23%). Strong correlations were found between PDFF and SS ($r_s=0.84$, $p<0.001$) or HFF (r_s
25 $=0.87$, $p<0.001$) (Figure 2). These two Spearman’s coefficients increased to 0.88 and 0.94 when
26 selecting only the patients without liver iron overload and decreased to 0.74 and 0.72 for the
27 patients with liver iron overload. The Bland and Altman analysis between PDFF and HFF found
28 a mean difference of 5.2 ± 4.9 (CI95% 4.6, 5.7) , 4.7 ± 3.7 (CI95% 4.2, 5.3) and 7.1 ± 8.8 (CI95%
29 5.2, 9.0) for all patients with HFF measurement, those without and those with liver iron
30 overload, respectively (Figure 3). The most discordant values appeared when the MR–LIC was
31 greater than 300 $\mu\text{mol/g}$ (Figure 4).
32
33
34
35
36
37
38
39
40
41

42 For the patients without liver iron overload having an HFF measurement, there was no
43 significant difference between 1.5T (n=102) and 3T (n=105) or between the 6 MR devices used
44 for these patients (Figure 5).
45
46
47
48

49 In the subgroup of 43 patients with a comparison of the PDFF obtained with the body coil and
50 phased-array coils, 6 patients had a slight hemosiderosis with a median MR–LIC of 43 $\mu\text{mol/g}$
51 (38-102 $\mu\text{mol/g}$). The linear regression coefficient between the two PDFF results was 0.995
52 with a slope of 1 and an intercept of 0.5% (Figure 6). The mean difference was $0.7\% \pm 0.7\%$
53 [CI95% 0.5%, 0.9%]. In the same subgroup, also examined using VIBE q-Dixon sequences 4
54 subjects, without liver iron overload, were excluded for implausible PDFF value above 60%.
55 For the remaining patients the linear regression coefficient was 0.99 with a slope of 1.1 and an
56
57
58
59
60
61
62
63
64
65

1 intercept of 0.4%. The mean difference was $1.9\% \pm 1.3\%$ [CI95% 1.5%, 2.4%]. When using
2 instead the data from the WIP-VIBE q-Dixon sequence there was no implausible PDFF. The
3 linear regression coefficient was 0.96 with a slope of 1.1 and an intercept of 0.68% (Figure 6).
4 The mean difference was $2.7\% \pm 2.3\%$ [CI95% 2.0%, 3.4%].
5
6
7
8

9 **Discussion**

10
11
12 The PDFF obtained by the 2D CSE–MRI sequence, using the body coil, analyzed by the
13 MRQuantif software, is very well correlated with the steatosis score ($r_s=0.84$) and with the
14 percentage of the total area of the fat vacuoles relative to the surface of the histological fragment
15 ($r_s=0.87$), particularly when considering patients without liver iron overload ($r_s=0.94$),
16
17
18
19
20
21

22 The quantification of hepatic steatosis by calculating the PDFF has already been validated by
23 numerous studies and has become a recognized biomarker. Most MRI manufacturers propose
24 a dedicated 3D sequence (IDEAL IQ from GE, mDIXON-Quant from Philips, VIBE q-Dixon
25 from the Siemens LiverLab package). However, most MRI scanners can also perform a 2D
26 CSE–MRI sequence with the basic configuration, but a post-processing software is then
27 required. In the literature Spearman’s correlation coefficient between PDFF and steatosis score
28 was lower or equal to our results, between 0.64 and 0.87 [24–29]. Most of these published
29 studies involved fewer than 100 subjects.
30
31
32
33
34
35
36
37

38 The quality of the comparison between MR and histology is also limited by the use of the semi-
39 quantitative steatosis cores. The subjective character of the measurement is responsible for
40 inter-observer or even intra-observer variability [30]. Above all, this measurement does not
41 relate to the same physical quantity as PDFF: in MRI a signal proportion is calculated while in
42 the steatosis score a percentage of distribution is estimated, without considering the size of the
43 fat vacuoles. Together with the limited used of liver biopsy, this explains why the PDFF was
44 more frequently compared with spectroscopy [13, 17, 18]. Results are then excellent, but it is
45 more a comparison of two MRI methods than a real comparison to liver steatosis.
46
47
48
49
50
51
52
53

54 Morphometric analysis of the histological image allows a quantitative evaluation of liver fat
55 fraction with a greater precision and reproducibility than steatosis score [31, 32]. It also
56 analyses the same physical quantity because the proportion in surface is similar to the
57
58
59
60
61
62
63
64
65

1 proportion in volume. Previous studies comparing histomorphometry or stereological
2 measurement and fat fraction obtained by spectroscopy or 2D CSE MR sequences have shown
3 a strong correlation [33–38]. Small differences in a few cases can be explained by the sampling
4 effect due to the small size of the biopsy core.
5
6

7
8
9 In our study, PDFF is very well correlated but gives a higher value, the mean bias is about 5%,
10 compared to HFF. This could be due to the difficulty of the histomorphometric analysis when
11 taking into account the surface of the micro vacuoles that are too small to be quantified. This
12 bias is of course reduced for PDFF below 5%. Another explanation is that PDFF is a signal
13 fraction and not stricto sensu a volume fraction.
14
15
16

17
18
19 To jointly quantify the iron concentration of the liver, the team from the University of Rennes
20 recommends the use of the body coil to allow the comparison of the signal from the liver and
21 the paraspinal muscles and thus avoid an underestimation of $R2^*$ in case of high iron overload.
22 The body coil provides a weaker signal in comparison to phased-array coils but it does not
23 affect performance. The reproducibility of the measurement between the two coils is quite
24 perfect. The selected 2D sequence, originally designed to quantify liver iron, probably has less
25 signal than a 3D sequence. However, the choice of a long TR, thick 2D slices and a low matrix,
26 made it possible to keep a high SNR, even with the body coil. Thus, no difference was observed
27 with 1.5T MRIs despite their lower SNR. This sequence was easy to implement on the 11
28 devices used in this study, without each center needing to purchase an expensive option.
29
30
31
32
33
34
35
36
37
38

39
40 Iron has a significant influence on the estimation of PDFF in these series. In cases of high
41 hepatic iron overload, the rapid decrease in hepatic signal can disrupt the PDFF estimation. In
42 our series, the major errors occurred when MR–LIC was above 300 $\mu\text{mol/g}$. Thus, a joint MR–
43 LIC estimation is recommended to ensure the validity of the PDFF obtained.
44
45
46
47
48
49
50

51 The results obtained with the dedicated Siemens sequence are also similar, with a slightly higher
52 value in the event of a high level of steatosis. The complexity of complex-based reconstruction
53 explains the few miscalculations of the VIBE q-Dixon post-processing. The improved
54 algorithm for water/fat identification in the WIP version of this sequence avoids these errors.
55 This is not an issue with magnitude-based methods but, on the other hand, they could lead to
56
57
58
59
60
61
62

1
2 ambiguity if the fat fraction is greater than 50%. However, such a high concentration is quite
3 exceptional.
4

5 The slope observed between PDFF and SS suggests that, on average, the latter, which was used
6 until now by hepatologists, is three times higher than PDFF. However, it would probably be
7 preferable to no longer rely on the histological score and to categorize the patients or to evaluate
8 the therapeutic efficacy on the PDFF, which is easier to acquire, more precise and more
9 reproducible.
10
11
12
13
14
15

16 To our knowledge, this is the largest series comparing the PDFF with liver biopsy and
17 especially with a large cohort of histomorphometric analyses. The multicenter recruitment, with
18 a great variability of the MR devices, makes it possible to definitely validate the evaluation of
19 the PDFF by the method initially proposed by the University of Rennes to quantify liver iron.
20
21
22
23
24

25 However, due to the retrospective combination of several studies and the multicentric nature of
26 one of them, the methodology is not perfectly homogeneous. Histomorphometry was not
27 available for all patients. Sequence comparison is limited to the last study and to one center. A
28 broader complementary comparison between MRQuantif and dedicated sequence from several
29 vendors is needed.
30
31
32
33
34
35

36 **Conclusion**

37

38
39 The PDFF provided by the MRQuantif software, analyzing 2D CSE–MR data, is well correlated
40 to the intrahepatic fat fraction obtained by the histomorphometry analysis, except when MR–
41 LIC was above 300 $\mu\text{mol/g}$. This sequence, available in the basic configuration on most MRI
42 scanners, associated with this software available online, can be useful for carrying out studies
43 using with several devices, particularly if they do not all have the vendor’s specific option.
44
45
46
47
48
49
50
51
52
53
54
55
56
57
58
59
60
61
62
63
64
65

1
2
3
4
5
6
7
8
9
10
11
12
13
14
15
16
17
18
19
20
21
22
23
24
25
26
27
28
29
30
31
32
33
34
35
36
37
38
39
40
41
42
43
44
45
46
47
48
49
50
51
52
53
54
55
56
57
58
59
60
61
62
63
64
65

Acknowledgements

Thanks to Stephan Kannengiesser (Siemens) for his useful comments.

Funding

SURFER and FibroMR research studies were funded by the French “Programme Hospitalier de Recherche Clinique” (PHRC)
SNIFF cohort was funded by Centre Hospitalier Universitaire of Angers

Compliance with Ethical Standards

Guarantor:

The scientific guarantor of this publication is GANDON Y.

Conflict of Interest:

The authors of this manuscript declare no relationships with any companies whose products or services may be related to the subject matter of the article.

Statistics and Biometry:

No complex statistical methods were necessary for this paper.

Informed Consent:

Written informed consent was obtained from all patients in this study.

Ethical Approval:

Institutional Review Board approval was obtained.

Study subjects or cohorts overlap:

Some other data of these study subjects or cohorts have been previously reported in several papers but never PDF data.

Methodology

- prospective
- diagnostic or prognostic study
- multicenter study

References

1. Bellentani S, Scaglioni F, Marino M, Bedogni G (2010) Epidemiology of non-alcoholic fatty liver disease. *Dig Dis Basel Switz* 28:155–161. <https://doi.org/10.1159/000282080>
2. Younossi ZM, Koenig AB, Abdelatif D et al (2016) Global epidemiology of nonalcoholic fatty liver disease-Meta-analytic assessment of prevalence, incidence, and outcomes. *Hepatology* 64:73–84. <https://doi.org/10.1002/hep.28431>
3. Tapper EB, Lok AS-F (2017) Use of Liver Imaging and Biopsy in Clinical Practice. *N Engl J Med* 377:756–768. <https://doi.org/10.1056/NEJMra1610570>
4. Rockey DC, Caldwell SH, Goodman ZD et al (2009) Liver biopsy. *Hepatology* 49:1017–1044. <https://doi.org/10.1002/hep.22742>
5. Kleiner DE, Brunt EM, Van Natta M et al (2005) Design and validation of a histological scoring system for nonalcoholic fatty liver disease. *Hepatology* 41:1313–1321. <https://doi.org/10.1002/hep.20701>
6. Hussain HK, Chenevert TL, Londy FJ et al (2005) Hepatic fat fraction: MR imaging for quantitative measurement and display--early experience. *Radiology* 237:1048–1055. <https://doi.org/10.1148/radiol.2373041639>
7. Li M, Song J, Mirkov S et al (2011) Comparing morphometric, biochemical, and visual measurements of macrovesicular steatosis of liver. *Hum Pathol* 42:356–360. <https://doi.org/10.1016/j.humpath.2010.07.013>
8. Boursier J, Chaigneau J, Roullier V et al (2011) Steatosis degree, measured by morphometry, is linked to other liver lesions and metabolic syndrome components in patients with NAFLD. *Eur J Gastroenterol Hepatol* 23:974–981. <https://doi.org/10.1097/MEG.0b013e32834a4d82>
9. Bohte AE, van Werven JR, Bipat S, Stoker J (2011) The diagnostic accuracy of US, CT, MRI and ¹H-MRS for the evaluation of hepatic steatosis compared with liver biopsy: a meta-analysis. *Eur Radiol* 21:87–97. <https://doi.org/10.1007/s00330-010-1905-5>
10. Szczepaniak LS, Nurenberg P, Leonard D et al (2005) Magnetic resonance spectroscopy to measure hepatic triglyceride content: prevalence of hepatic steatosis in the general population. *Am J Physiol Endocrinol Metab* 288:E462-468. <https://doi.org/10.1152/ajpendo.00064.2004>
11. Reeder SB, Sirlin CB (2010) Quantification of liver fat with magnetic resonance imaging. *Magn Reson Imaging Clin N Am* 18:337–357, ix. <https://doi.org/10.1016/j.mric.2010.08.013>
12. Hamilton G, Yokoo T, Bydder M et al (2011) In vivo characterization of the liver fat ¹H MR spectrum. *NMR Biomed* 24:784–790. <https://doi.org/10.1002/nbm.1622>
13. Yokoo T, Shieh-morteza M, Hamilton G et al (2011) Estimation of hepatic proton-density fat fraction by using MR imaging at 3.0 T. *Radiology* 258:749–759. <https://doi.org/10.1148/radiol.10100659>

14. Yu H, Shimakawa A, McKenzie CA et al (2008) Multiecho water-fat separation and simultaneous R2* estimation with multifrequency fat spectrum modeling. *Magn Reson Med* 60:1122–1134. <https://doi.org/10.1002/mrm.21737>
15. Reeder SB, Robson PM, Yu H et al (2009) Quantification of hepatic steatosis with MRI: the effects of accurate fat spectral modeling. *J Magn Reson Imaging JMRI* 29:1332–1339. <https://doi.org/10.1002/jmri.21751>
16. Yokoo T, Bydder M, Hamilton G et al (2009) Nonalcoholic fatty liver disease: diagnostic and fat-grading accuracy of low-flip-angle multiecho gradient-recalled-echo MR imaging at 1.5 T. *Radiology* 251:67–76. <https://doi.org/10.1148/radiol.2511080666>
17. Heba ER, Desai A, Zand KA et al (2016) Accuracy and the effect of possible subject-based confounders of magnitude-based MRI for estimating hepatic proton density fat fraction in adults, using MR spectroscopy as reference. *J Magn Reson Imaging JMRI* 43:398–406. <https://doi.org/10.1002/jmri.25006>
18. Zand KA, Shah A, Heba E et al (2015) Accuracy of multiecho magnitude-based MRI (M-MRI) for estimation of hepatic proton density fat fraction (PDFF) in children. *J Magn Reson Imaging JMRI* 42:1223–1232. <https://doi.org/10.1002/jmri.24888>
19. Gu J, Liu S, Du S et al (2019) Diagnostic value of MRI-PDFF for hepatic steatosis in patients with non-alcoholic fatty liver disease: a meta-analysis. *Eur Radiol* 29:3564–3573. <https://doi.org/10.1007/s00330-019-06072-4>
20. Qu Y, Li M, Hamilton G et al (2019) Diagnostic accuracy of hepatic proton density fat fraction measured by magnetic resonance imaging for the evaluation of liver steatosis with histology as reference standard: a meta-analysis. *Eur Radiol* 29:5180–5189. <https://doi.org/10.1007/s00330-019-06071-5>
21. Gu Q, Cen L, Lai J et al (2021) A meta-analysis on the diagnostic performance of magnetic resonance imaging and transient elastography in nonalcoholic fatty liver disease. *Eur J Clin Invest* 51:e13446. <https://doi.org/10.1111/eci.13446>
22. Yokoo T, Serai SD, Pirasteh A et al (2018) Linearity, Bias, and Precision of Hepatic Proton Density Fat Fraction Measurements by Using MR Imaging: A Meta-Analysis. *Radiology* 286:486–498. <https://doi.org/10.1148/radiol.2017170550>
23. Hu HH, Yokoo T, Bashir MR et al (2021) Linearity and Bias of Proton Density Fat Fraction as a Quantitative Imaging Biomarker: A Multicenter, Multiplatform, Multivendor Phantom Study. *Radiology* 298:640–651. <https://doi.org/10.1148/radiol.2021202912>
24. Tang A, Desai A, Hamilton G et al (2015) Accuracy of MR imaging-estimated proton density fat fraction for classification of dichotomized histologic steatosis grades in nonalcoholic fatty liver disease. *Radiology* 274:416–425. <https://doi.org/10.1148/radiol.14140754>
25. Idilman IS, Aniktar H, Idilman R et al (2013) Hepatic steatosis: quantification by proton density fat fraction with MR imaging versus liver biopsy. *Radiology* 267:767–775. <https://doi.org/10.1148/radiol.13121360>

- 1
2
3
4
5
6
7
8
9
10
11
12
13
14
15
16
17
18
19
20
21
22
23
24
25
26
27
28
29
30
31
32
33
34
35
36
37
38
39
40
41
42
43
44
45
46
47
48
49
50
51
52
53
54
55
56
57
58
59
60
61
62
63
64
65
26. Parente DB, Rodrigues RS, Paiva FF et al (2014) Is MR spectroscopy really the best MR-based method for the evaluation of fatty liver in diabetic patients in clinical practice? *PloS One* 9:e112574. <https://doi.org/10.1371/journal.pone.0112574>
 27. Boudinaud C, Abergel A, Joubert-Zakeyh J et al (2019) Quantification of steatosis in alcoholic and nonalcoholic fatty liver disease: Evaluation of four MR techniques versus biopsy. *Eur J Radiol* 118:169–174. <https://doi.org/10.1016/j.ejrad.2019.07.025>
 28. Hwang I, Lee JM, Lee KB et al (2014) Hepatic steatosis in living liver donor candidates: preoperative assessment by using breath-hold triple-echo MR imaging and ¹H MR spectroscopy. *Radiology* 271:730–738. <https://doi.org/10.1148/radiol.14130863>
 29. Kühn J-P, Evert M, Friedrich N et al (2011) Noninvasive quantification of hepatic fat content using three-echo dixon magnetic resonance imaging with correction for T2* relaxation effects. *Invest Radiol* 46:783–789. <https://doi.org/10.1097/RLI.0b013e31822b124c>
 30. El-Badry AM, Breitenstein S, Jochum W et al (2009) Assessment of hepatic steatosis by expert pathologists: the end of a gold standard. *Ann Surg* 250:691–697. <https://doi.org/10.1097/SLA.0b013e3181bcd6dd>
 31. Franzén LE, Ekstedt M, Kechagias S, Bodin L (2005) Semiquantitative evaluation overestimates the degree of steatosis in liver biopsies: a comparison to stereological point counting. *Mod Pathol Off J U S Can Acad Pathol Inc* 18:912–916. <https://doi.org/10.1038/modpathol.3800370>
 32. Rawlins SR, El-Zammar O, Zinkievich JM et al (2010) Digital quantification is more precise than traditional semiquantitation of hepatic steatosis: correlation with fibrosis in 220 treatment-naïve patients with chronic hepatitis C. *Dig Dis Sci* 55:2049–2057. <https://doi.org/10.1007/s10620-010-1254-x>
 33. Longo R, Pollesello P, Ricci C et al (1995) Proton MR spectroscopy in quantitative in vivo determination of fat content in human liver steatosis. *J Magn Reson Imaging JMRI* 5:281–285. <https://doi.org/10.1002/jmri.1880050311>
 34. Nasr P, Forsgren MF, Ignatova S et al (2017) Using a 3% Proton Density Fat Fraction as a Cut-Off Value Increases Sensitivity of Detection of Hepatic Steatosis, Based on Results From Histopathology Analysis. *Gastroenterology* 153:53-55.e7. <https://doi.org/10.1053/j.gastro.2017.03.005>
 35. Galimberti S, Trombini P, Bernasconi DP et al (2015) Simultaneous liver iron and fat measures by magnetic resonance imaging in patients with hyperferritinemia. *Scand J Gastroenterol* 50:429–438. <https://doi.org/10.3109/00365521.2014.940380>
 36. Cesbron-Métivier E, Roullier V, Boursier J et al (2010) Noninvasive liver steatosis quantification using MRI techniques combined with blood markers. *Eur J Gastroenterol Hepatol* 22:973–982. <https://doi.org/10.1097/meg.0b013e32833775fb>
 37. Jayakumar S, Middleton MS, Lawitz EJ et al (2019) Longitudinal correlations between MRE, MRI-PDFF, and liver histology in patients with non-alcoholic steatohepatitis: Analysis of data from a phase II trial of selonsertib. *J Hepatol* 70:133–141. <https://doi.org/10.1016/j.jhep.2018.09.024>

38. St Pierre TG, House MJ, Bangma SJ et al (2016) Stereological Analysis of Liver Biopsy Histology Sections as a Reference Standard for Validating Non-Invasive Liver Fat Fraction Measurements by MRI. PloS One 11:e0160789. <https://doi.org/10.1371/journal.pone.0160789>

Figure legends

Figure 1: Screen copy of the placement of ROIs using MRQuantif software viewer (L1, L2, L3 for liver; M1, M2 for paraspinal muscle; N1 for background noise).

Figure 2: Linear correlation between PDFF and histology for all patients, but also dissociating patients without (plotted in blue) or with (plotted in red) liver iron overload.

(a) Correlation between PDFF and steatosis score (SS).

(b) Correlation between PDFF and histology fat fraction (HFF).

Figure 3: Bland and Altman analysis exploring the mean FF (%) difference between 2D CSE–MR sequence PDFF and HFF.

(a) Analysis of all patients (patients with liver iron overload are plotted in red).

(b) Selection of patients without liver iron overload.

Solid line represents the bias, dashed lines represent the upper and lower limits of agreement.

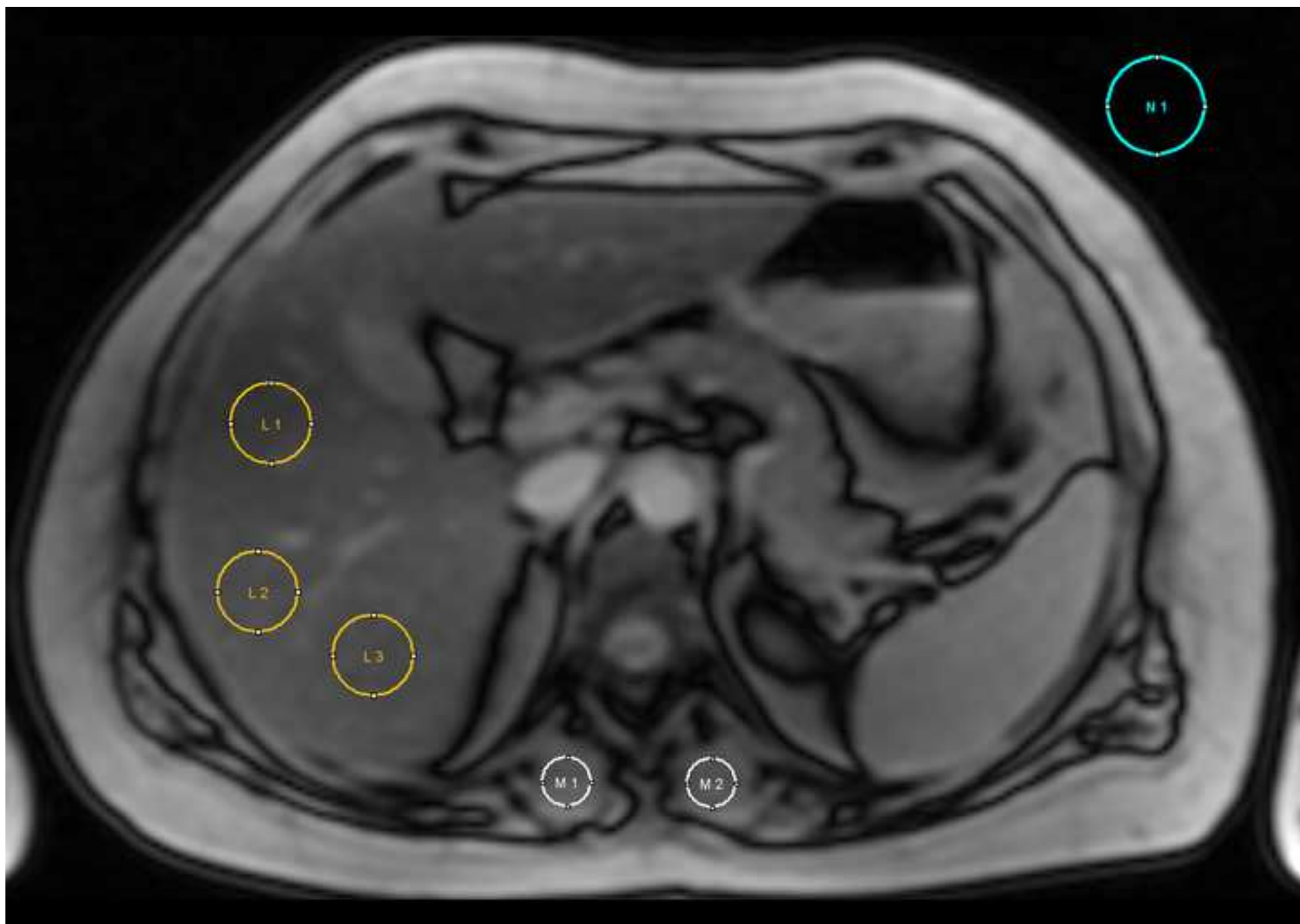
Figure 4: Differences between PDFF and HFF plotted against MR–LIC (patients with liver iron overload are plotted in red). A greater lack of agreement appeared when MR–LIC increased above $300\mu\text{mol/g}$.

Figure 5: Linear correlation between PDFF and HFF for the patients without liver iron overload.

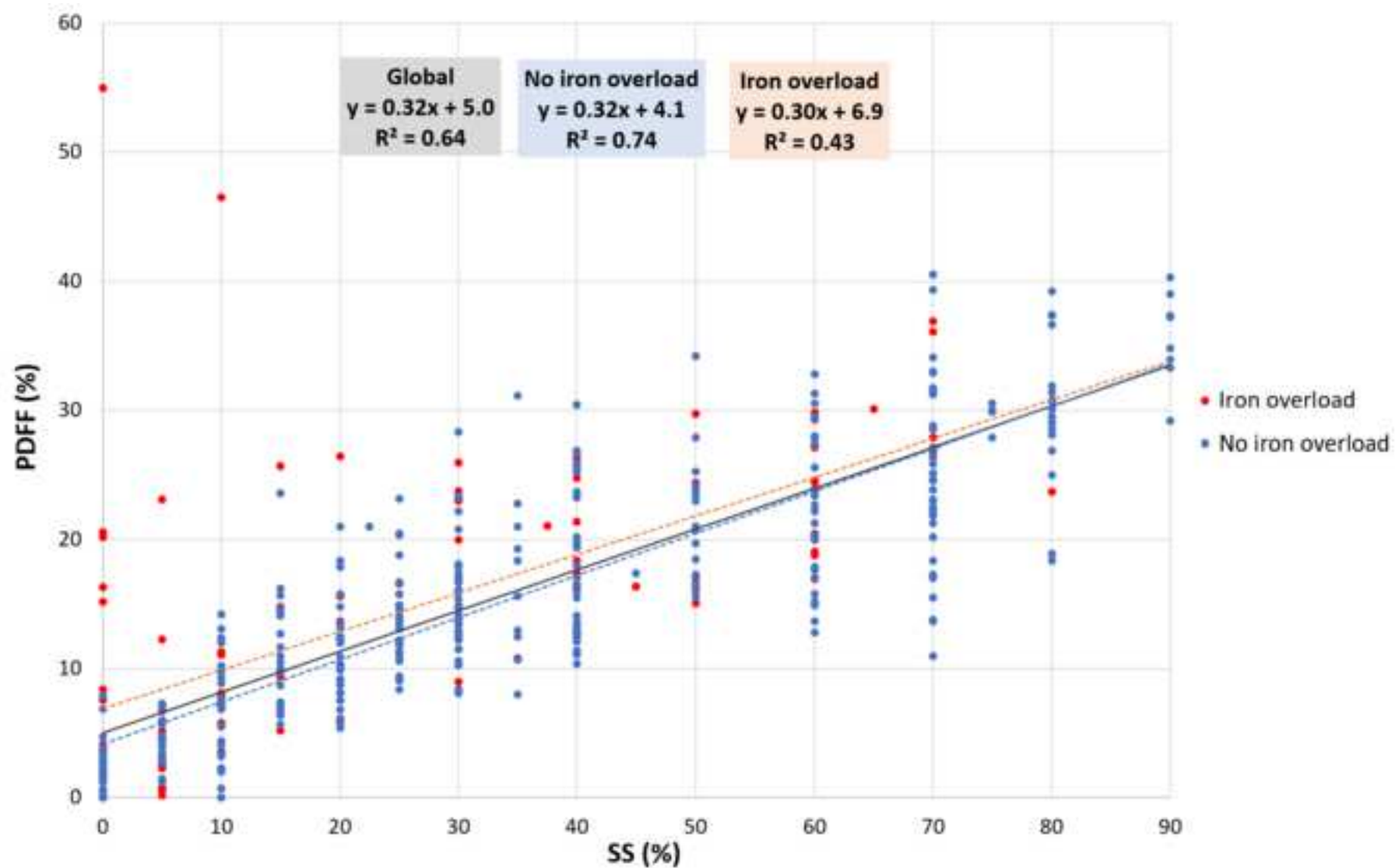
(a) Comparison of 1.5T and 3T systems.

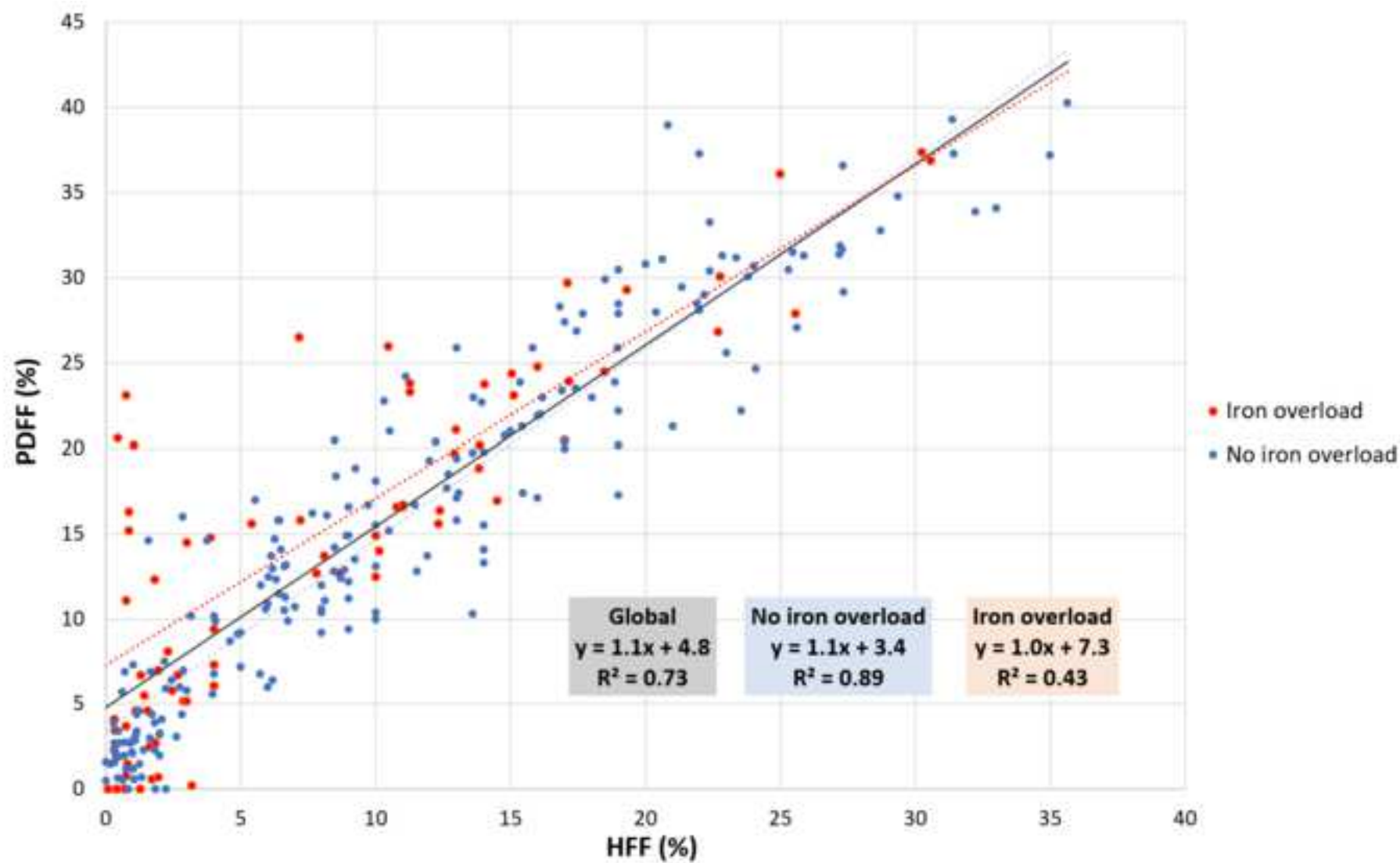
(b) Comparison of the 6 devices used in this group of patients with HFF measurement.

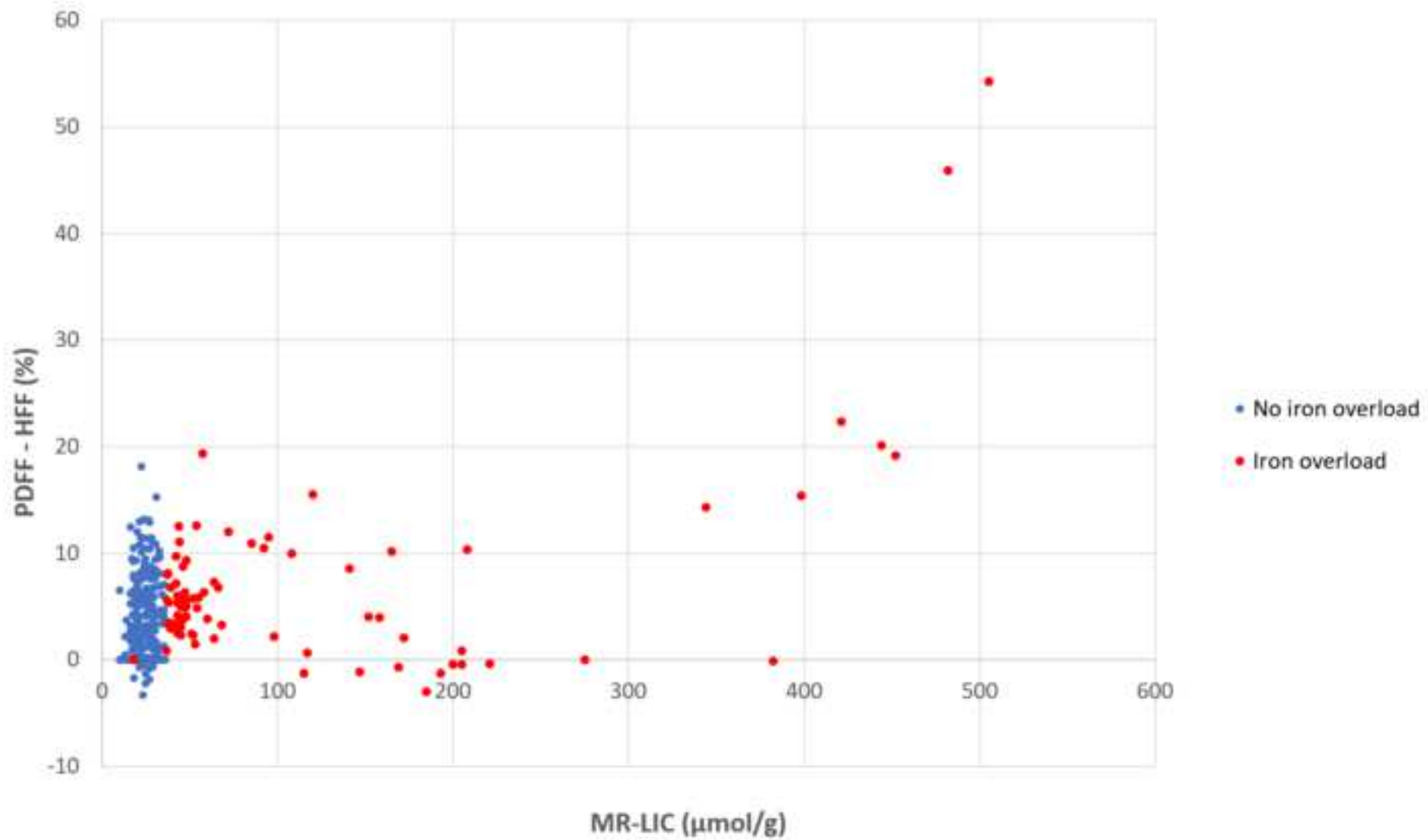
Figure 6: Linear correlation of PDFF obtained from 2D CSE–MR sequence by body coil and phased-array coil (patients with liver iron overload are plotted in red).

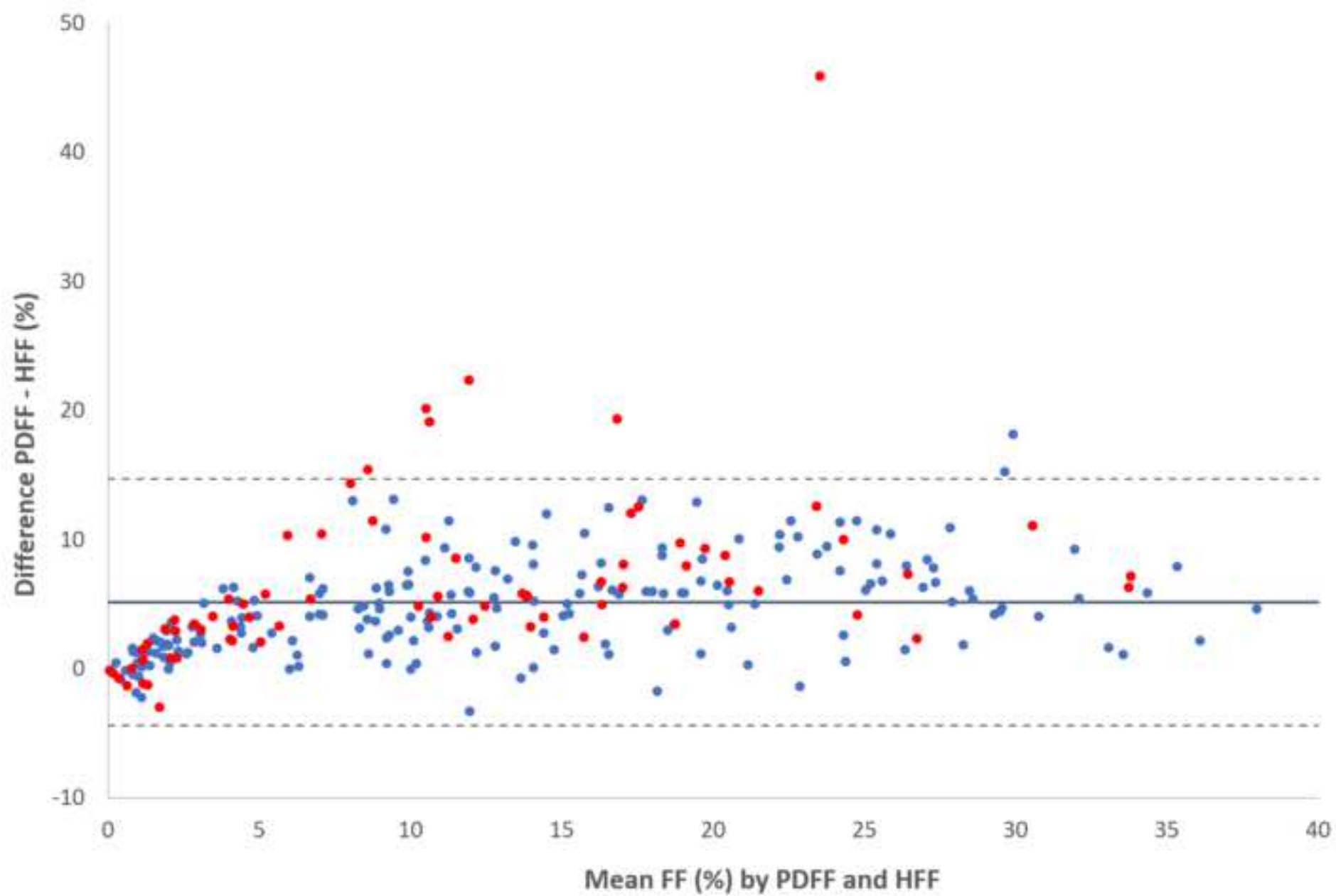


Accepted manuscript

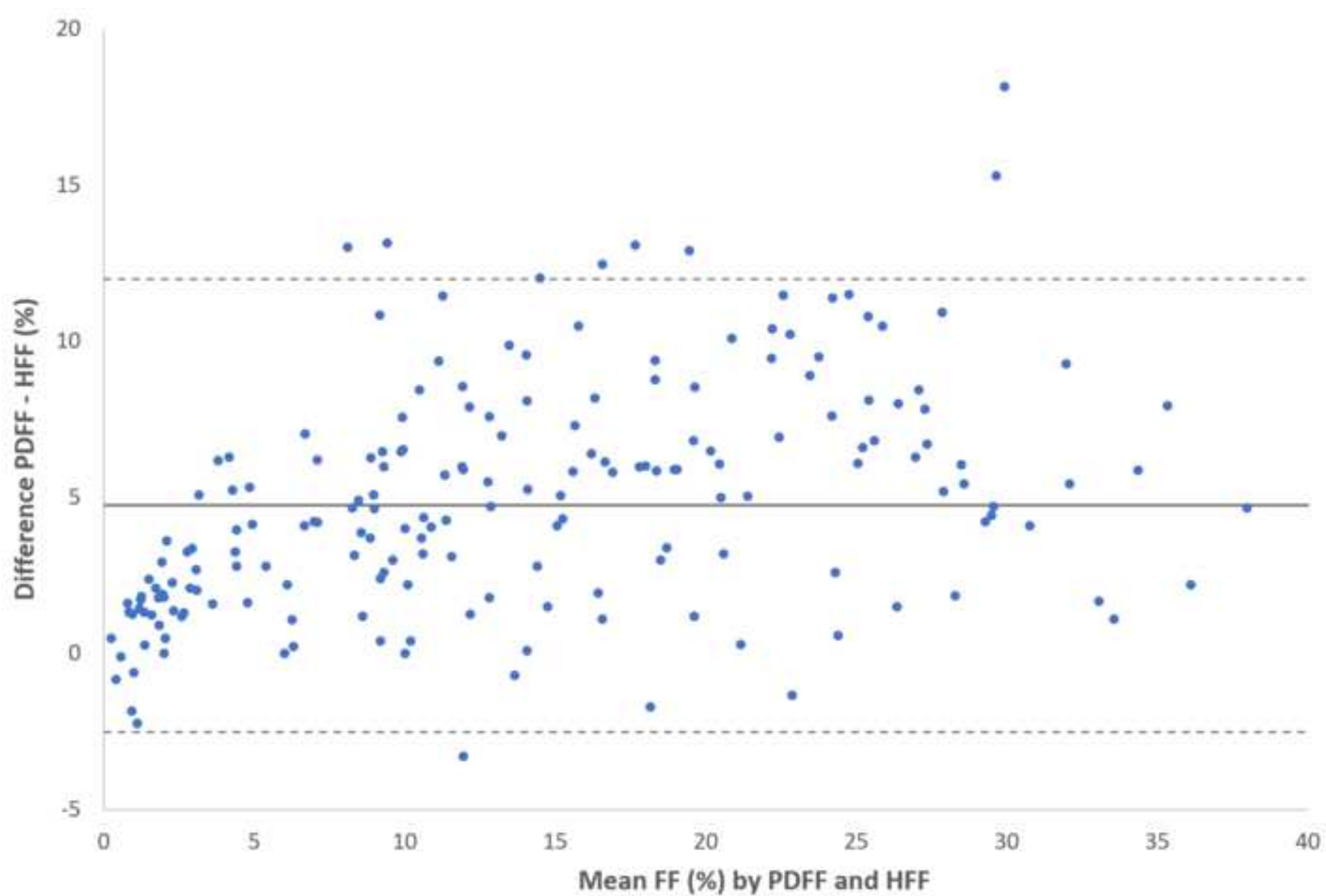




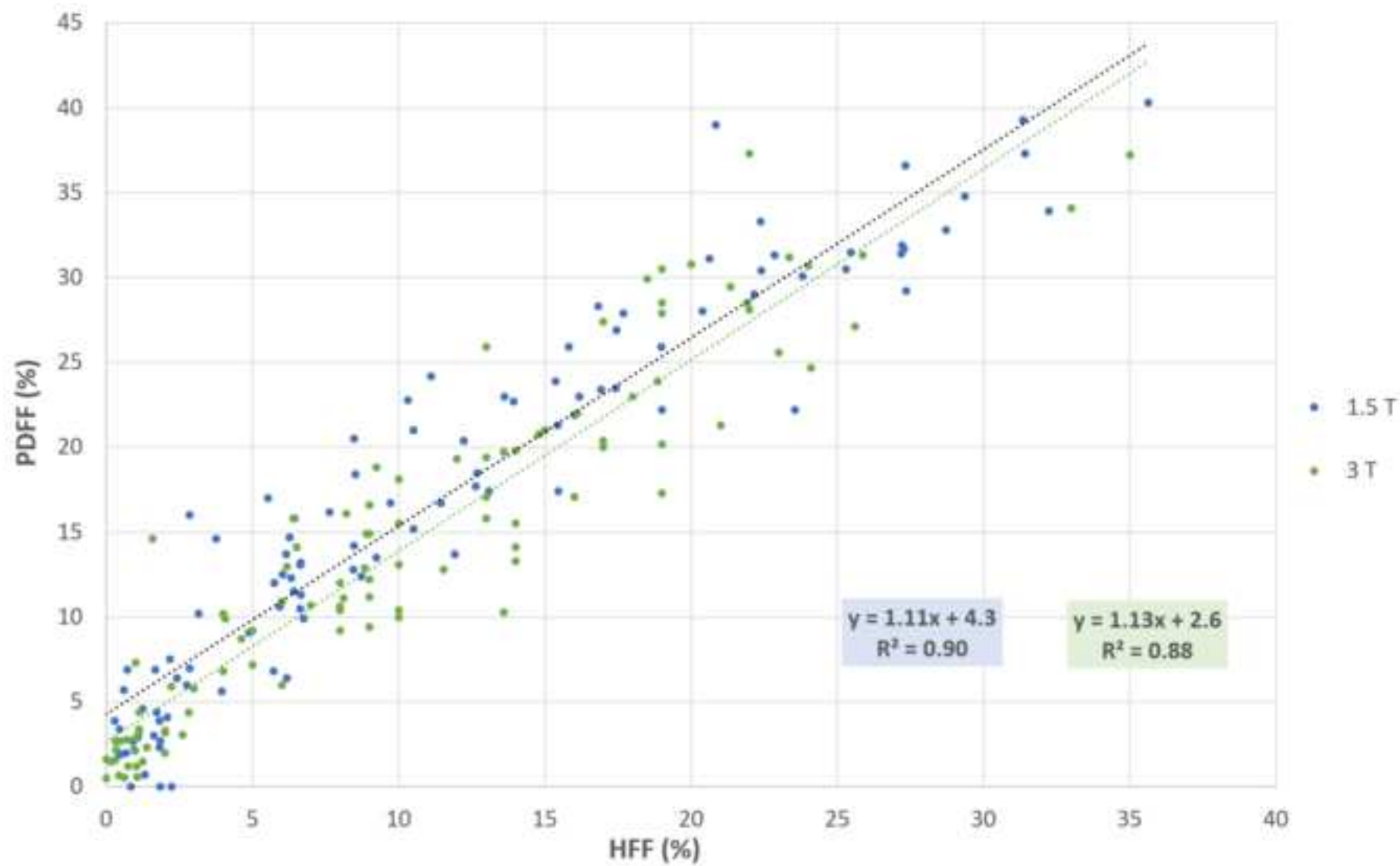


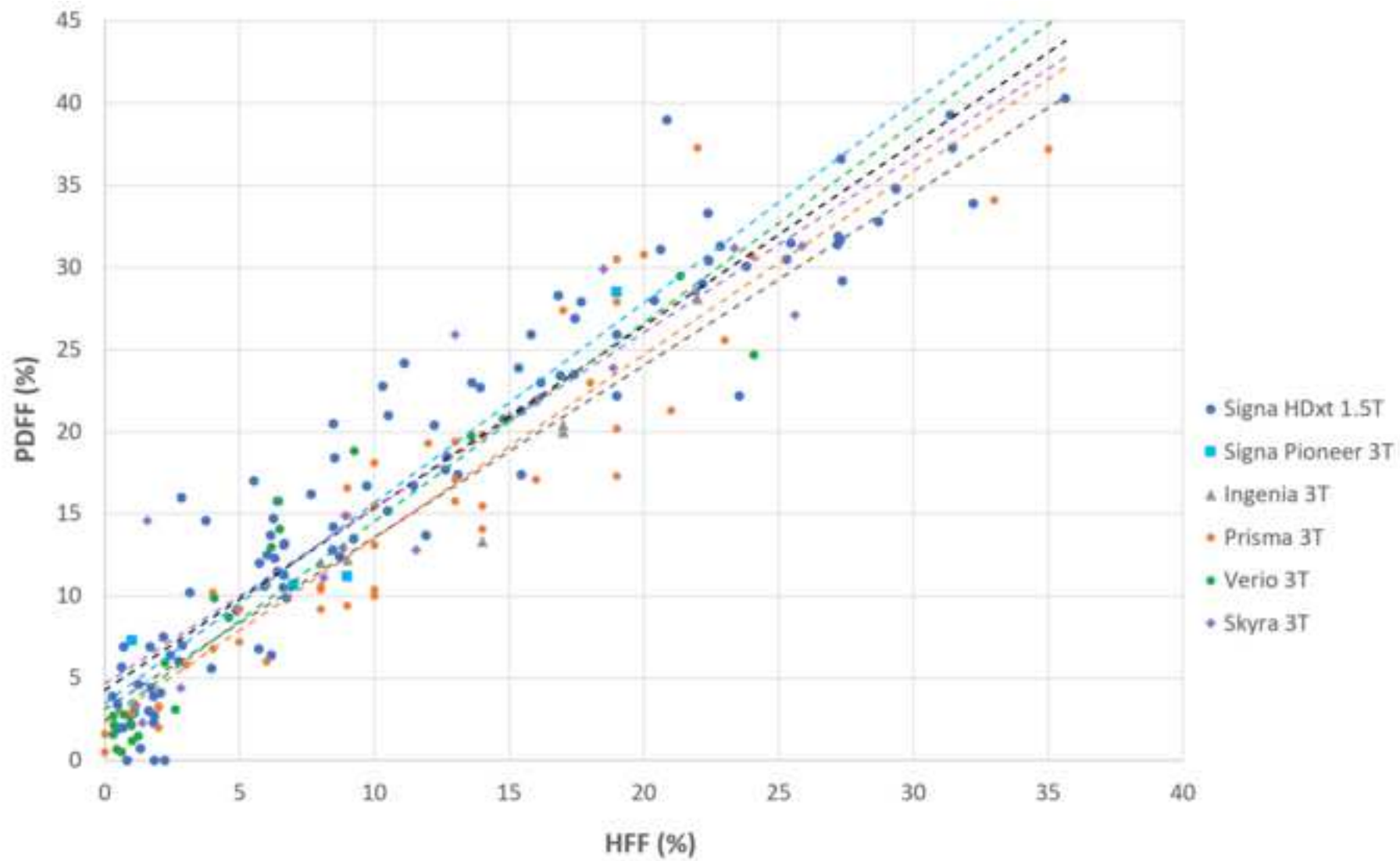


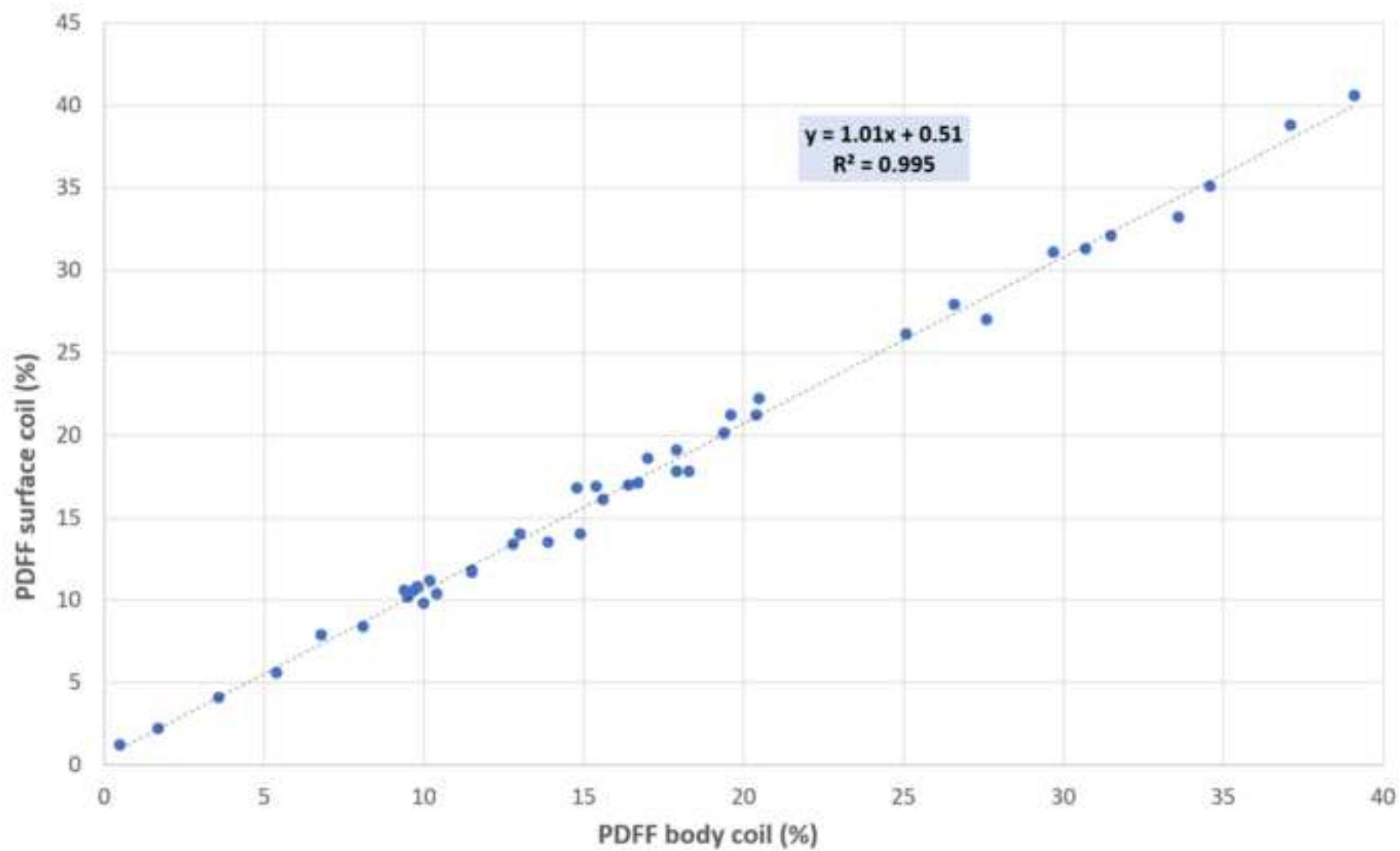
Accepted manuscript



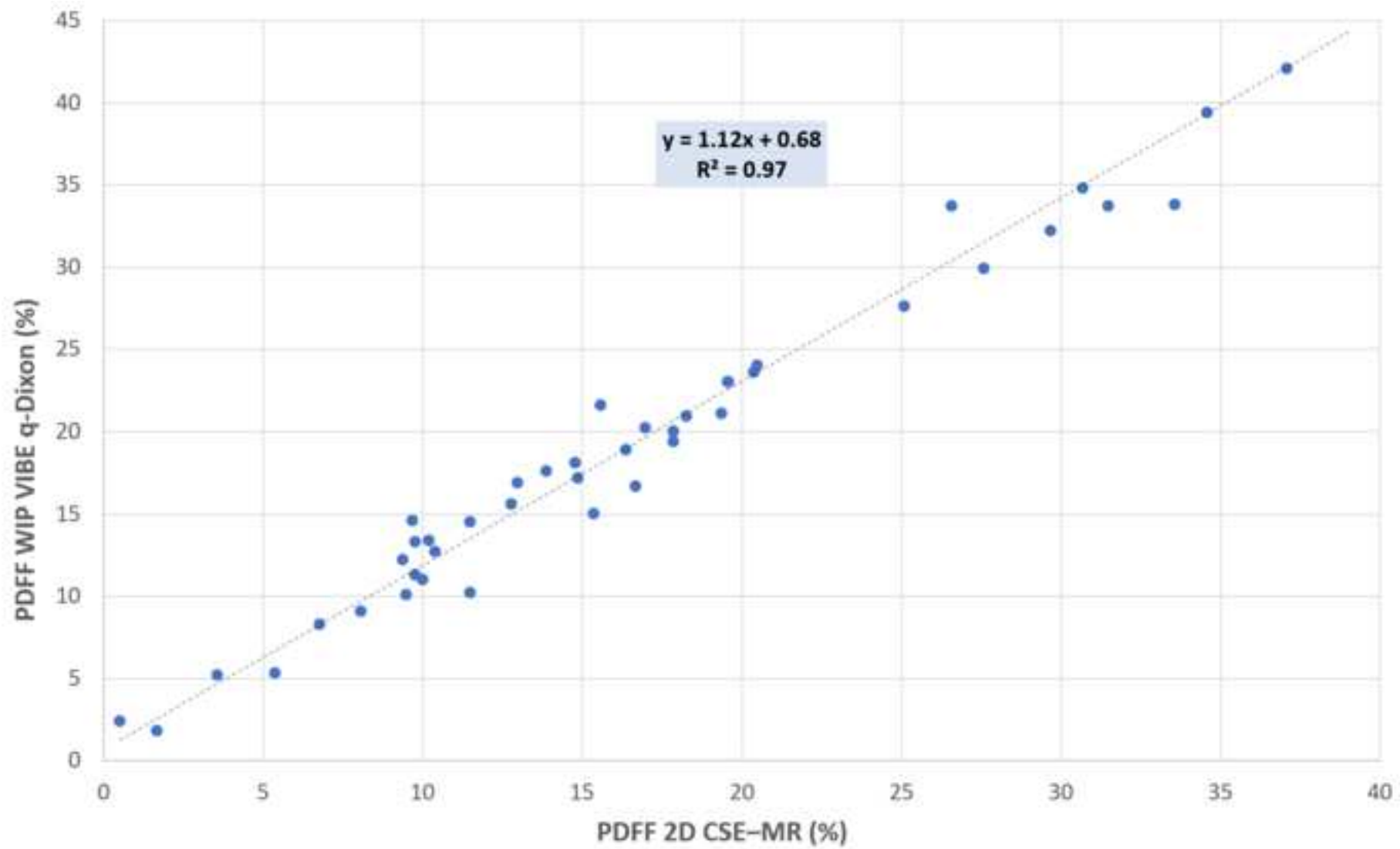
Accepted manuscript







Accepted manuscript



Accepted manuscript

Acknowledgements

Thanks to Stephan Kannengiesser (Siemens) for his useful comments.

Funding

SURFER and FibroMR research studies were funded by the French “Programme Hospitalier de Recherche Clinique” (PHRC)
SNIFF cohort was funded by Centre Hospitalier Universitaire of Angers

Compliance with Ethical Standards***Guarantor:***

The scientific guarantor of this publication is GANDON Y.

Conflict of Interest:

The authors of this manuscript declare no relationships with any companies whose products or services may be related to the subject matter of the article.

Statistics and Biometry:

No complex statistical methods were necessary for this paper.

Informed Consent:

Written informed consent was obtained from all patients in this study.

Ethical Approval:

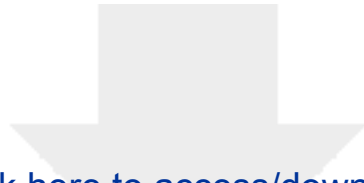
Institutional Review Board approval was obtained.

Study subjects or cohorts overlap:

Some other data of these study subjects or cohorts have been previously reported in several papers but never PDF data.

Methodology

- prospective
- diagnostic or prognostic study
- multicenter study

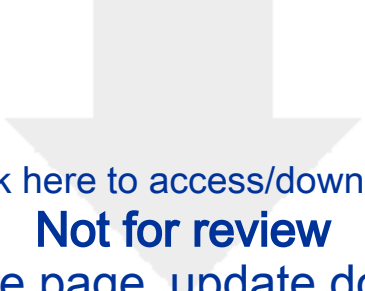


Click here to access/download

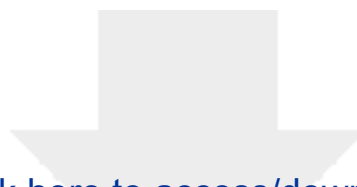
Supplementary Material

EURA-D-22-03700_supplementary material.pdf





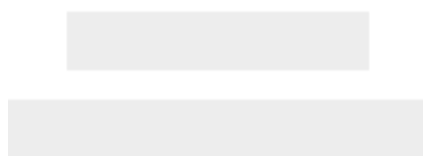
[Click here to access/download](#)
Not for review
[Title page_update.docx](#)

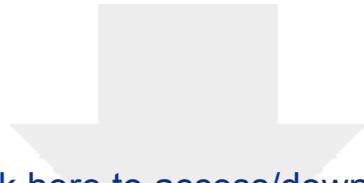


[Click here to access/download](#)

Not for review

EURA-D-22-03700R2_ANNOTATED.docx

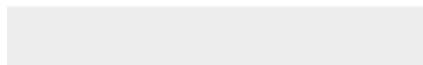
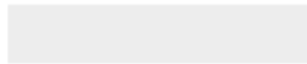


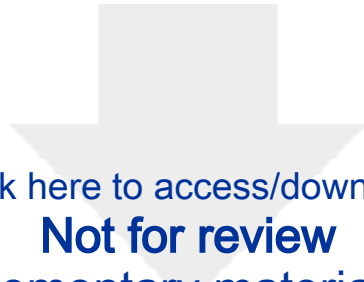


[Click here to access/download](#)

Not for review

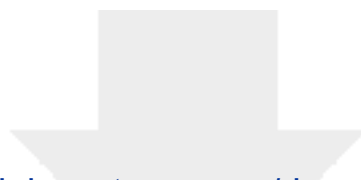
[Disclosure-Paragraph-template_NEW.docx](#)





Click here to access/download
Not for review
Supplementary material.docx

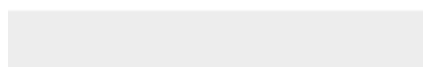
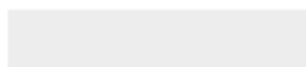




[Click here to access/download](#)

Not for review

EURA-D-22-03700R2_CLEAN.docx

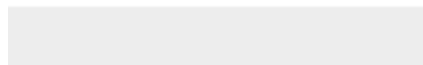


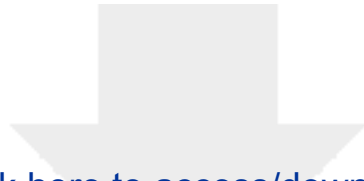


[Click here to access/download](#)

Not for review

[EURA-D-22-03700R1_WithCRS.docx](#)

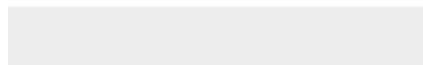


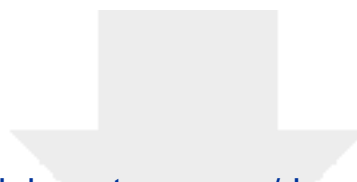


[Click here to access/download](#)

Not for review

Title page_Corrected.docx

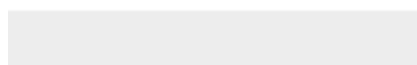
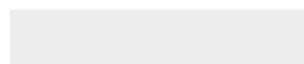




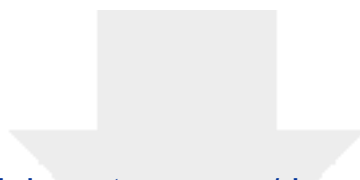
[Click here to access/download](#)

Not for review

[EURA-D-22-03700R1_ANSWERS.docx](#)







[Click here to access/download](#)

Not for review

EURA-D-22-03700R1_CLEAN.docx

